Interaction of light with an atom near the surface of a superlattice. I. Periodic case

Xiao-shen Li
Shanghai Institute of Metallurgy, Academia Sinica, 865 Chang Ning Road, Shanghai 200 050, People's Republic of China and International Center for Materials Physics, Academia Sinica, Shenyang, Liaoning, People's Republic of China

Chang-de Gong
Center of Theoretical Physics, Chinese Center of Advanced Science and Technology (World Laboratory), 52 Sanlihe Road, P.O. Box 8730, Beijing 100 080, Beijing, People's Republic of China and Department of Physics, Nanjing University, Nanjing, Jiangsu, People's Republic of China
(Received 13 May 1988)

Luminescence properties and resonance fluorescence for an adatom near the surface of a semi-infinite periodic superlattice are investigated by means of surface-dressed optical Bloch equations and Maxwell's equations. The effects of dielectric properties and thicknesses of the layers composing this superlattice are discussed and some novel phenomena are discovered.

I. INTRODUCTION

Interesting phenomena related to the interaction of electromagnetic field with atoms or molecules absorbed near solid surfaces include surface-enhanced Raman scattering,[1-13] coherence and energy transfer in spontaneous emission,[14-33] and surface-induced resonance fluorescence spectrum.[34-40] These luminescence and scattering properties for adsorbed species on solid surface, which provide a sensitive probe of the electronic and other structure of the solid substrates, prompted a careful reexamination of the optics of surfaces. Once the mechanisms of these optical processes are fully understood and brought under experimental control, they will become a powerful tool for the analysis of surface process.

Nearly two decades ago, the perfection of the fatty-acid monolayer assembly technique[41,42] led to a series of successful measurements on the luminescent lifetime of excited molecules near gold, silver, and copper surfaces.[14,43,44] It was found that for large distances from the metal surface the luminescent lifetime of the molecules oscillates as a function of distance, while for short distances it tends monotonically to zero.[22] Kuhn provided explanations for these experimental results by using a modified image theory.[16] Within the framework of this theory, the molecule as an oscillating dipole located near a partially reflecting mirror was coupled with its image. The interference between the electric field emitted by the image dipole and the initial field gives rise to the observed oscillations in the lifetime. The decrease of the lifetime in short distances is due to nonradiative energy transfer from the molecule to the surface. Many papers focusing on the energy-transfer problem for various surfaces provided theoretical results[17,18,20,22,28] and experimental observations,[14,29,30,32,33,43,44] with the former in good agreement with the latter. Many quantum-mechanical treatments of this problem have also appeared.[15,19,21,24]

Morawitz[15] used the image method to obtain the spontaneous decay rate and frequency shift for a two-level atom near a perfect-conductor surface, from both a quantum-mechanical viewpoint and a classical one. This quantum-mechanical approach was later generalized by Milonni and Knight[21] to discuss luminescence of an atom between two infinite-plane mirrors parallel to each other. Agarwal and co-workers[19,24] developed a linear-response theory to discuss the coherence in spontaneous emission of an atom located in the vicinity of a solid surface. Very recently, Liu and George[31] proposed a quantum-mechanical version of the image method to study the spontaneous emission by two atoms with different resonant frequencies near a perfectly conducting metal surface.

On the other hand, when an atom is driven by a strong driving coherent field with frequency nearly on resonance with the adatomic transition frequency, the external field puts the atom in an environment where the probability of stimulated emission may exceed that of spontaneous emission. In this case, ac Stark splitting and Rabi oscillations of probability amplitudes of the atomic levels and nutational oscillations of the emitted-field intensity become pronounced, so that resonance fluorescence,[45-47] squeezing,[48] and other nonlinear-optical phenomena can occur.[49,50] In these light-driving processes, multiphoton processes[51] become as important as single-photon ones, so the low-order perturbation method is no longer reliable. In the surface-free case, these processes can be effectively dealt with by using the well-known optical Bloch equations (OBE) for atoms in gases[46,47,52] or in low-temperature solids.[53,54] Very recently, a set of surface-dressed optical Bloch equations (SBE) for an adatom near a solid surface were derived by Huang, George, and co-workers[34-39,55] to discuss the effects of the surface-reflected photons, the resonance interaction be-

tween the adatom and surface plasmons, the collision dephasing of the adatom produced by gas atoms in the medium, and the random-phase fluctuation of the intense laser field. In their discussions they studied the resonance fluorescence for an adatom at a flat metal surface in the case of weak excitation[34] or strong excitation[35] and for an adatom at a rough metal surface[38,39] which was modeled as a hemispheroid protrusion on a perfectly conducting surface. On the other hand, Li and Gong[40] provided another set of SBE through a different procedure including Dekker's quantization procedure for a dissipative system.[56,57] They discussed the resonance fluorescence for an adatom near a surface of a perfect conductor or a dielectric with transverse frequency coinciding with that of the adatomic transition, taking into account the size and dielectric effects of a supporting dielectric layer.

In this paper we study the luminescence properties and resonance fluorescence for an adatom near a surface of a semi-infinite superlattice through using the SBE (Ref. 40) and Maxwell's equations. This superlattice is composed of two constituents. The adatom is taken as an emitting dipole from which the electromagnetic field is emitted. This field is reflected by the surface and interfaces of the superlattice and coupled back with the dipole of which the dynamic behavior is thus influenced. We are interested in the effects of the dielectric properties and the thickness of each layer on the optical properties of this adatom. The outline of this paper is as follows. In Sec. II we use Maxwell's equations to calculate the reflected field determining the SBE. In Sec. III we study the spontaneous decay rate and frequency shift through numerical calculations. In Secs. IV, V, and VI, we consider that the adatom is irradiated by an external laser field and discuss resonance fluorescence spectrum, time evolution of the population inversion, and fluctuations of the dipole moment, respectively. In Sec. VII we give some concluding remarks.

II. REFLECTED FIELD AND SBE FOR A SUPERLATTICE SURFACE

There is considerable interest in the properties of superlattices[58–62] composed generally of alternating layers of different materials. Here we consider the typical case[61] that a semi-infinite superlattice has two constituents, of which one is called material A with thickness d_A and dielectric constant ϵ_A, and the other called material B with d_B and ϵ_B, as shown in Fig. 1. There is an atom or a dipole with moment $\mathbf{p}$ located at a distance d from the surface of this superlattice. Similar to Ref. 40, first we may use Maxwell's equations and corresponding boundary conditions to find the reflected electric field at the dipole position.

First, as in Refs. 19 and 40, we consider the general case that there is an emitting dipole located at $\mathbf{r}=\mathbf{r}_0$ in the semi-infinite region $z<0$ with dielectric constant ϵ. The other half-space is composed of the alternating layers of two materials A and B.

From Maxwell's equations

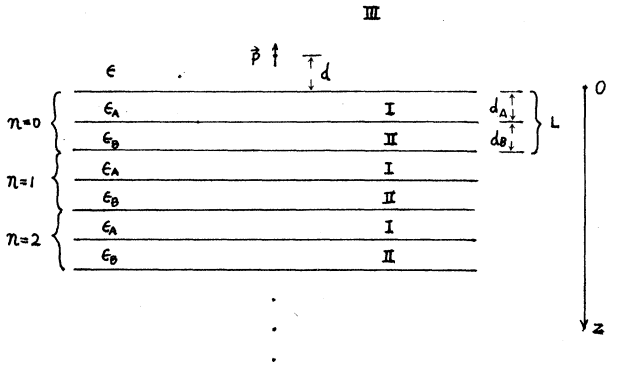

FIG. 1. An adatom with electric moment $\mathbf{p}$ is located at a distance d from a surface of a semi-infinite superlattice occupying region $z>0$.

$$\begin{aligned}
&\nabla\times\mathbf{E}=\frac{1}{c}\frac{\partial}{\partial t}\mathbf{B}\ ,\\
&\nabla\times\mathbf{B}=0\ ,\\
&\nabla\times\mathbf{H}=\frac{1}{c}\frac{\partial}{\partial t}(\mathbf{D}+4\pi\mathcal{P})\ ,\\
&\nabla\cdot(\mathbf{D}+4\pi\mathcal{P})=0\ ,
\end{aligned}\tag{2.1}$$

and the expression for the dipole moment

$$\mathcal{P}(\mathbf{r},\omega)=\mathbf{p}(\omega)\delta(\mathbf{r}-\mathbf{r}_0)\ ,\tag{2.2}$$

we obtain the following set of equations:[19,40]

$$\nabla^2\mathbf{E}_A+\epsilon_A k_0^2\mathbf{E}_A=0,\quad \nabla\cdot\mathbf{E}_A=0$$
$$\mathbf{H}_A=\nabla\times\mathbf{E}_A/ik_0\quad \text{for } nL<z<nL+d_1\ ;\tag{2.3}$$
$$\nabla^2\mathbf{E}_B+\epsilon_B k_0^2\mathbf{E}_B=0,\quad \nabla\cdot\mathbf{E}_B=0$$
$$\mathbf{H}_B=\nabla\times\mathbf{E}_B/ik_0\quad \text{for } nL+d_1<z<(n+1)L\ ;\tag{2.4}$$
$$\nabla^2\mathbf{E}+\epsilon k_0^2\mathbf{E}=-4\pi[k_0^2\mathcal{P}+\epsilon^{-1}\nabla(\nabla\cdot\mathcal{P})]\ ,$$
$$\mathbf{H}=\nabla\times\mathbf{E}/ik_0\quad \text{for } z<0\ .\tag{2.5}$$

Noticing the periodic structure of the semi-infinite superlattice, similar to Ref. 61, the electric field in this superlattice may have a Bloch-wave-like form with an envelope function decaying exponentially as one goes into the superlattice. Thus we have the solution for the electric field of Eqs. (2.3)–(2.5):[19,40,61]

$$\begin{aligned}
\mathbf{E}_A(\mathbf{r},\omega)=&\int\int\exp(i\mathbf{k}_\parallel\cdot\mathbf{r}-\beta nL)\\
&\times\{\mathcal{E}_A^{(+)}(u,v,\omega)\exp[iw_A(z-nL)]\\
&+\mathcal{E}_A^{(-)}(u,v,\omega)\\
&\times\exp[-iw_A(z-nL)]\}du\,dv\ ,\\
&\mathbf{k}_A\cdot\mathcal{E}_A^{(+)}=0,\quad \mathbf{k}'_A\cdot\mathcal{E}_A^{(-)}=0,\quad \mathbf{k}_A=(k_\parallel,w_A)\ ,\\
&\mathbf{k}'_A=(k_\parallel,-w_A),\quad w_A^2=\epsilon_A k_0^2-k_\parallel^2\ ,\\
&\mathbf{k}_\parallel=(u,v,0)\quad \text{for } nL<z<nL+d_1\ ;
\end{aligned}\tag{2.6}$$

$$\mathbf{E}_B(\mathbf{r},\omega)=\int\int \exp(i\mathbf{k}_\parallel\cdot\mathbf{r}-\beta nL)\times\{\mathcal{E}_B^{(+)}(u,v,\omega)\exp[iw_B(z-nL-d_1)]+\mathcal{E}_B^{(-)}(u,v,\omega)\times\exp[-iw_B(z-nL-d_1)]\}du\,dv\ ,$$

$$\mathbf{k}_B\cdot\mathcal{E}_B^{(+)}=0,\quad \mathbf{k}'_B\cdot\mathcal{E}_B^{(-)}=0,\quad \mathbf{k}_B=(k_\parallel,w_B)\ ,$$

$$\mathbf{k}'_B=(k_\parallel,-w_B),\quad w_B^2=\epsilon_B k_0^2-k_\parallel^2 \quad \text{for } nL+d_1<z<(n+1)L\ ; \tag{2.7}$$

$$\mathbf{E}(\mathbf{r},\omega)=\int\int \exp(i\mathbf{k}_\parallel\cdot\mathbf{r}-iwz)\mathcal{E}(u,v,\omega)du\,dv+\mathbf{E}_p(\mathbf{r},\omega)\ ,$$

$$\mathbf{k}'\cdot\mathcal{E}=0,\quad \mathbf{k}'=(k_\parallel,-w),\quad w^2=\epsilon k_0^2-k_\parallel^2 \quad \text{for } \mathrm{Im}w\geq 0 \text{ and } z<0\ , \tag{2.8}$$

where $\mathrm{Re}\beta\geq 0$, the subscript $\parallel$ means parallel to the interfaces, and

$$\mathbf{E}_p(\mathbf{r},\omega)=-(2\pi i)^{-1}\times\int\int w^{-1}[k_0^2\mathbf{p}+\epsilon^{-1}\nabla(\mathbf{p}\cdot\nabla)]\times\exp[iu(x-x_0)+iv(y-y_0)+iw|z-z_0|]du\,dv\ . \tag{2.9}$$

For simplicity, in what follows we shall consider the vertical orientation of the dipole.[38] Using (2.6) and (2.8) and applying the Maxwell boundary conditions at $z=0$, we obtain[19,40]

$$\mathbf{k}_\parallel\cdot\mathcal{E}_\parallel=\mathbf{k}_\parallel\cdot\mathcal{E}_{A\parallel}^{(+)}+\mathbf{k}_\parallel\cdot\mathcal{E}_{A\parallel}^{(-)}+\nu wk_\parallel^2 p\ , \tag{2.10}$$

$$\mathbf{k}_\parallel\cdot\mathcal{E}_\parallel=-(\epsilon_A w/\epsilon w_A)(\mathbf{k}_\parallel\cdot\mathcal{E}_{A\parallel}^{(+)}-\mathbf{k}_\parallel\cdot\mathcal{E}_{A\parallel}^{(-)})-\nu wk_\parallel^2 p\ , \tag{2.11}$$

where

$$\nu=-(2\pi i\epsilon w)^{-1}\exp(-i\mathbf{k}\cdot\mathbf{r}_0)\ . \tag{2.12}$$

In the same way, with (2.6) and (2.7) and the boundary conditions at $z=nL$ and $z=nL+d_1$, we obtain

$$\mathbf{k}_\parallel\cdot\mathcal{E}_{A\parallel}^{(+)}-\mathbf{k}_\parallel\cdot\mathcal{E}_{A\parallel}^{(-)}=(\epsilon_B w_A/\epsilon_A w_B)\times[\mathbf{k}_\parallel\cdot\epsilon_{B\parallel}^{(+)}\exp(iw_B d_B)-\mathbf{k}_\parallel\cdot\mathcal{E}_{B\parallel}^{(-)}\exp(-iw_B d_B)]\exp(\beta L)\ , \tag{2.13}$$

$$\mathbf{k}_\parallel\cdot\mathcal{E}_{A\parallel}^{(+)}+\mathbf{k}_\parallel\cdot\mathcal{E}_{A\parallel}^{(-)}=[\mathbf{k}_\parallel\cdot\mathcal{E}_{B\parallel}^{(+)}\exp(iw_B d_B)+\mathbf{k}_\parallel\cdot\mathcal{E}_{B\parallel}^{(-)}\exp(-iw_B d_B)]\exp(\beta L)\ , \tag{2.14}$$

and

$$\exp(iw_A d_A)\mathbf{k}_\parallel\cdot\mathcal{E}_{A\parallel}^{(+)}-\exp(-iw_A d_A)\mathbf{k}_\parallel\cdot\mathcal{E}_{A\parallel}^{(-)}=(\epsilon_B w_A/\epsilon_A w_B)(\mathbf{k}_\parallel\cdot\mathcal{E}_{B\parallel}^{(+)}-\mathbf{k}_\parallel\cdot\mathcal{E}_{B\parallel}^{(-)})\ , \tag{2.15}$$

$$\exp(iw_A d_A)\mathbf{k}_\parallel\cdot\mathcal{E}_{A\parallel}^{(+)}+\exp(-iw_A d_A)\mathbf{k}_\parallel\cdot\mathcal{E}_{A\parallel}^{(-)}=\mathbf{k}_\parallel\cdot\mathcal{E}_{B\parallel}^{(+)}+\mathbf{k}_\parallel\cdot\mathcal{E}_{B\parallel}^{(-)}\ , \tag{2.16}$$

respectively. Through similar procedure to Refs. 61 and 19, with Eqs. (2.10)–(2.16) we find the reflected electric field at the dipole position $(0,0,-d)$,

$$E_R=i\tfrac{3}{2}\epsilon^{-3/2}\gamma^0 pI/|p|^2\ , \tag{2.17}$$

where

$$I=\int_0^\infty dk\,k^3\exp(2iU\hat{d})\{-2(1-V_{AE})\exp(\beta L)+[(1-V_{BE})(1+V_{AB})\exp(iU_B\hat{d}_B)+(1+V_{BE})(1-V_{AB})\exp(-iU_B\hat{d}_B)]\exp(iU_A\hat{d}_A)\}\times U^{-1}\{2(1+V_{AE})\exp(\beta L)-[(1+V_{BE})(1+V_{AB})\exp(iU_B\hat{d}_B)+(1-V_{BE})(1-V_{AB})\exp(-iU_B\hat{d}_B)]\exp(iU_A\hat{d}_A)\}^{-1} \tag{2.18}$$

and $\exp(\beta L)$ is determined by the equation

$$e^{2\beta L}-\tfrac{1}{2}[(1+V_{AB})(1+V_{BA})\cos(U_A\hat{d}_A+U_B\hat{d}_B)+(1-V_{AB})(1-V_{BA})\cos(U_A\hat{d}_A-U_B\hat{d}_B)]e^{\beta L}+1=0\ ; \tag{2.19}$$

γ^0 ($=\frac{2}{3}\sqrt{\epsilon}|p|^2\omega^3/c^3$) is the decay rate in the absence of the surface[19,22,63] and we have defined

$$V_{AE}=\epsilon_A U/\epsilon U_A,\quad V_{BE}=\epsilon_B U/\epsilon U_B\ ,$$
$$V_{AB}=\epsilon_A U_B/\epsilon_B U_A,\quad V_{BA}=V_{AB}^{-1}\ , \tag{2.20}$$

where

$$U=(\epsilon-k^2)^{1/2},\quad U_A=(\epsilon_A-k^2)^{1/2}\ ,$$
$$U_B=(\epsilon_B-k^2)^{1/2},\quad k_0=\omega/c,\quad k=k_\parallel/k_0\ , \tag{2.21}$$
$$\hat{d}=\omega d/c,\quad \hat{d}_A=\omega d_A/c,\quad \hat{d}_B=\omega d_B/c\ .$$

From Eqs. (2.6) and (2.7) one may define a penetration depth

$$\hat{d}_\eta=nL=(\mathrm{Re}\beta)^{-1}\ . \tag{2.22}$$

We have found that the dependence of $\hat{d}_\eta$ on k is not very pronounced. So, we numerically calculated Eqs. (2.19) and (2.22) and some results are presented in Figs. 2 and 3. From these figures one can see the dependence of penetration depth on dielectric properties and thicknesses of the layers in the superlattice. Larger $\hat{d}_\eta$ means that the reflected field carries more informations about the

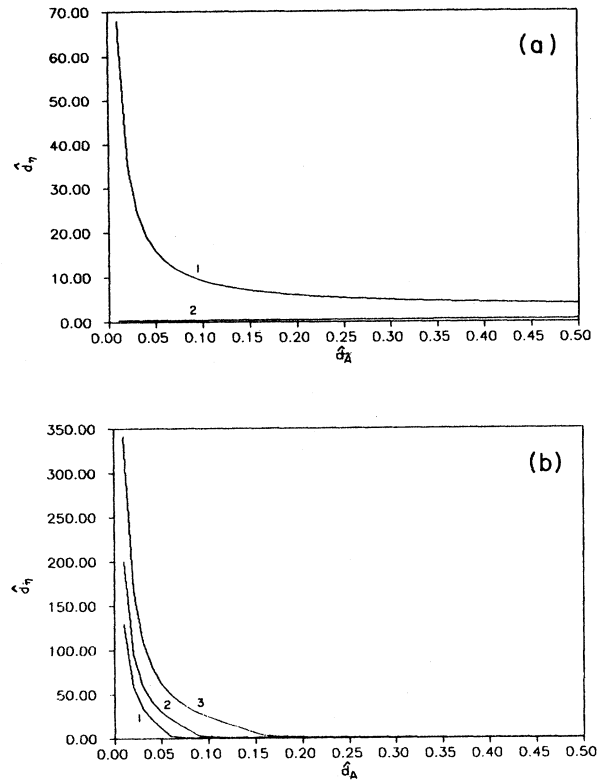

FIG. 2. Penetration depth $\hat{d}_\eta$ of electric field vs thickness of medium A: (a) $d_B=0.2$; curve 1, $\epsilon_A=1.96+1.06i$ (arachidic acid), $\epsilon_B=3.0$ (Al_2O_3); curve 2, $\epsilon_A=1.74$ (Na_3AlF_6), $\epsilon_B=17.05i$ (Fe); (b) $\epsilon_A=-10.5+0.5i$ (Ag), $\epsilon_B=3.0$ (Al_2O_3); curve 1, $\hat{d}_B=0.2$; curve 2, $\hat{d}_B=0.3$; curve 3, $\hat{d}_B=0.5$.

deep layers and vice versa.

In Ref. 40 we have derived a set of new SBE by using Dekker's quantization procedure for a dissipation system[56,57] and the reservoir theory.[64] These new SBE are different from those in Refs. 34–39. The difference lies in the fact that in new SBE, the presence of the solid surface affects not only the phase decay rate but also the spontaneous decay rate and frequency shift. In the rotating frame the new SBE are[40]

$$\frac{d}{dt}\begin{bmatrix}\langle S^+\rangle\\ \langle S^z\rangle\\ \langle S^-\rangle\end{bmatrix}=\begin{bmatrix}i(\Delta+\Omega^s)-\gamma & i\Omega & 0\\ i\Omega^*/2 & -2\gamma & -i\Omega/2\\ 0 & -i\Omega^* & -i(\Delta+\Omega^s)-\gamma\end{bmatrix}\times\begin{bmatrix}\langle S^+\rangle\\ \langle S^z\rangle\\ \langle S^-\rangle\end{bmatrix}-\begin{bmatrix}0\\ \gamma\\ 0\end{bmatrix}, \tag{2.23}$$

where the total decay rate $\gamma=\gamma^0+\gamma^s$, detuning $\Delta=\omega_{21}-\omega_L$, Rabi frequency $\Omega=|p|E$; $\gamma^s=|p|^2\mathrm{Im}f(d)$ and $\Omega^s=|p|^2\mathrm{Re}f(d)$ are the surface-induced spontaneous decay rate and frequency shift, respectively; ω_{21} is the adatomic transition frequency, $|p|$ the matrix element of electric dipole operator, ω_L and E the frequency and amplitude of the external laser field, respectively; $f(d)$ is a function of the distance d and determined by[40]

$$E_R=|p|f(d)S^-=pf(d)\ , \tag{2.24}$$

where E_R is the component of $\mathbf{E}_R$ in the direction of $\mathbf{p}$.

With the SBE (2.23) and the expression for the reflected field E_R, we can study the interaction between radiation fields and the adatom.

III. SPONTANEOUS DECAY RATE AND FREQUENCY SHIFT

With Eqs. (2.17), (2.18), and (2.24), we can obtain the spontaneous decay rate and frequency shift in the unit of γ^0 for an adatom near this superlattice surface,

$$\gamma=1+\tfrac{3}{2}\epsilon^{-3/2}\mathrm{Re}I\ , \tag{3.1}$$

$$\Omega^s=-\tfrac{3}{2}\epsilon^{-3/2}\mathrm{Im}I\ . \tag{3.2}$$

With numerical methods we have analyzed the effects of dielectric properties and the size of the layers composing this superlattice on γ and Ω^s. Some of the results are shown in Figs. 4–6, where $\epsilon=1.2$ and $\hat{d}=0.3$. From these figures one can see that the spontaneous emission properties of the adatom carry information about the properties and structure of the superlattice substrate. Figure 4 shows that when medium A is a metal and B is a nonabsorbing dielectric, the γ-$\hat{d}_A$ curve may have a peak resulting from the presence of the surface plasmon, and at the appearance of this peak the Ω^s-$\hat{d}_A$ curve has a steep slope. Figure 5 shows that the position, height, and half-width of this peak and the slope of the Ω^s-$\hat{d}_A$ curve strongly depend on the thickness of medium B. In addition, Fig. 4 also shows that when both A and B are dielectrics, the above phenomenon may disappear. Figure 6 shows that when medium A is a metal and B is a nonabsorbing dielectric, the γ-(ω/ω_p) curve has two peaks of which the height, position, and half-width depend on the thickness of each kind of layers, and at the appearance of these peaks $d\Omega^s/dx$ always takes negative values. This phenomenon is very similar to the absorption and dispersion phenomenon occurring in light transmitting through a medium. Of the above peaks, the

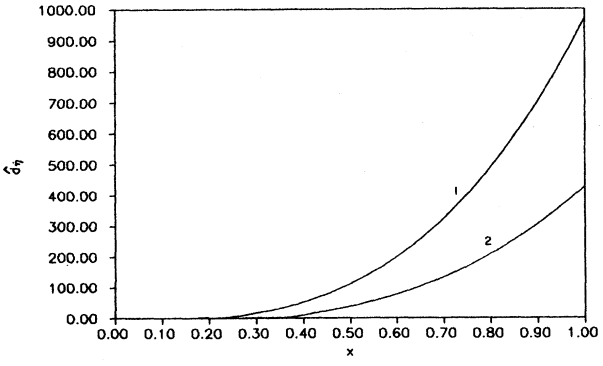

FIG. 3. Penetration depth $\hat{d}_\eta$ vs ratio of the adatomic transition frequency ω to the plasmon frequency ω_p of medium A containing a metal with dielectric function $\epsilon_A(\omega)=1-\omega_p^2/(\omega^2+i\omega\Gamma_p)$, $\Gamma_p=0.01\omega_p$, $x=\omega/\omega_p$, $\epsilon_B=3.0$, $\hat{d}_A=0.1$; curve 1, $\hat{d}_B=0.5$; curve 2, $\hat{d}_B=0.2$.

left one resulted from the presence of the surface plasmon absorbing energy from the excited adatom, while the right peak may result from the multibeam interference, since for larger ratio ω/ω_p the electric field can go very deep into the superlattice (see Fig. 3).

IV. RESONANCE FLUORESCENCE SPECTRUM

Here we consider that the two-level adatom near the superlattice surface is excited by an external laser field with amplitude E and frequency ω_L. Using the SBE (2.23), through the well-known procedure,[45,52,40] we can easily obtain the incoherent part of the resonance fluorescence spectrum related to the inelastic scattering between the laser and the adatom

$$\tilde{g}(\nu)=\frac{\frac{1}{2}|\Omega|^4\gamma(D^2+\frac{1}{2}|\Omega|^2+4\gamma^2)}{(X^2+Y^2)(\frac{1}{2}|\Omega|^2+|z|^2)} , \tag{4.1}$$

where

$$D=\nu-\omega_L,\quad z=\gamma+i(\Delta+\Omega^s) ,$$
$$X=2\gamma(\tfrac{1}{2}|\Omega|^2+|z|^2-2D^2) ,$$
$$Y=D(|\Omega|^2+|z|^2+4\gamma^2-D^2) .$$

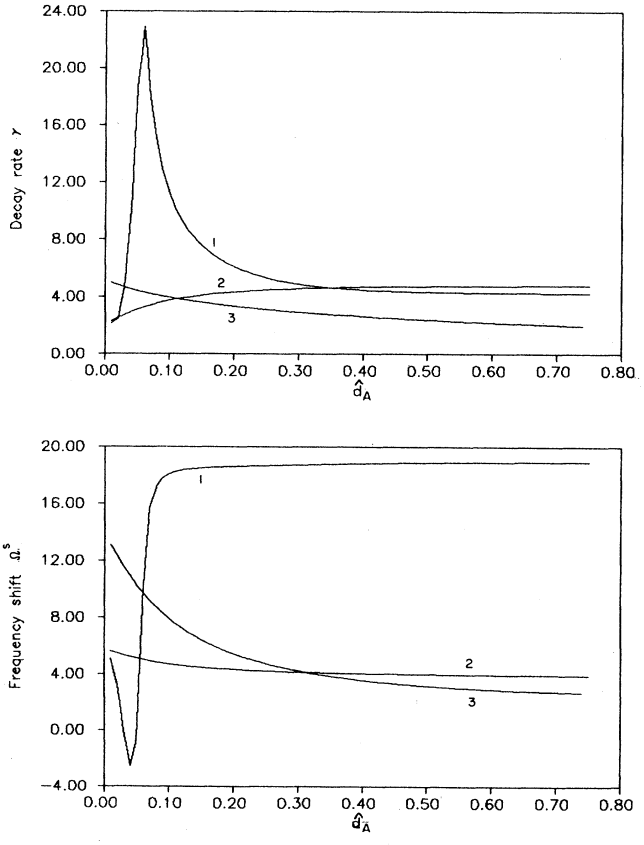

FIG. 4. Spontaneous decay rate γ and frequency shift Ω^s vs $\hat{d}_A$ for different materials; curve 1, $\epsilon_A=-10.5+0.5i$ (Ag), $\epsilon_B=3.0$ (Al_2O_3); curve 2, $\epsilon_A=1.96+1.06i$ (arachidic acid), $\epsilon_B=3.0$; curve 3, $\epsilon_A=1.74$ (Na_3AlF_6), $\epsilon_B=17.05i$ (Fe).

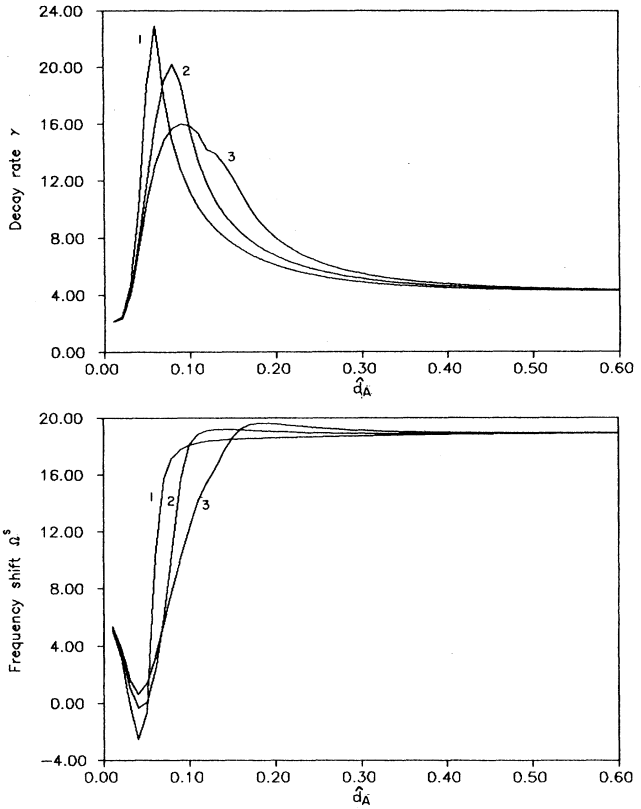

FIG. 5. Spontaneous decay rate γ and frequency shift Ω^s vs $\hat{d}_A$ for different thicknesses of medium B, $\epsilon_A=-10.5+0.5i$, $\epsilon_B=3.0$; curve 1, $\hat{d}_B=0.2$; curve 2, $\hat{d}_B=0.3$; curve 3, $\hat{d}_B=0.5$.

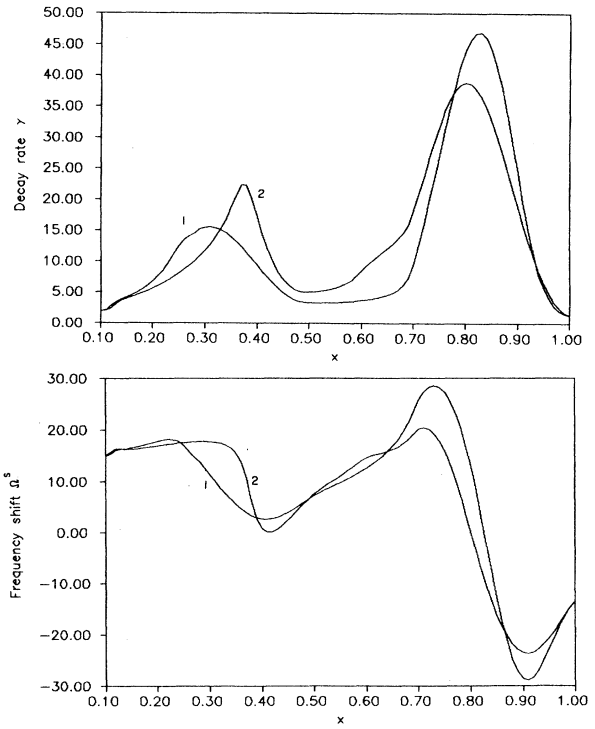

FIG. 6. γ and Ω_s vs x $(=\omega/\omega_p)$, $\epsilon_A=1-\omega_p^2/(\omega^2+i\omega\Gamma_p)$, $\Gamma_p=0.01\omega_p$, $\hat{d}_A=0.1$, $\epsilon_B=3.0$; curve 1, $\hat{d}_B=0.5$; curve 2, $\hat{d}_B=0.2$.

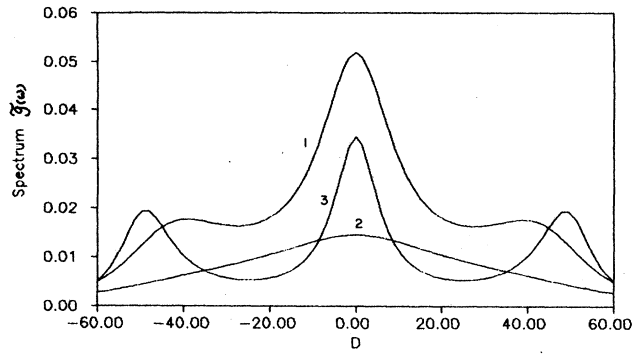

FIG. 7. Resonance fluorescence spectrum. $\Delta=2.0$, $|\Omega|=45.0$, $\epsilon_A=-10.5+0.5i$, $\epsilon_B=3.0$, $\hat{d}_B=0.2$. Curve 1, $\hat{d}_A=0.04$; curve 2, $\hat{d}_A=0.06$; curve 3, $\hat{d}_A=0.25$.

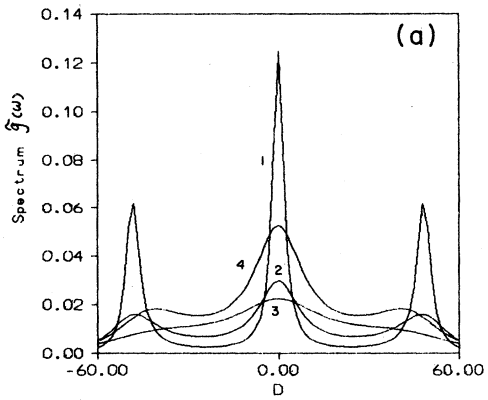

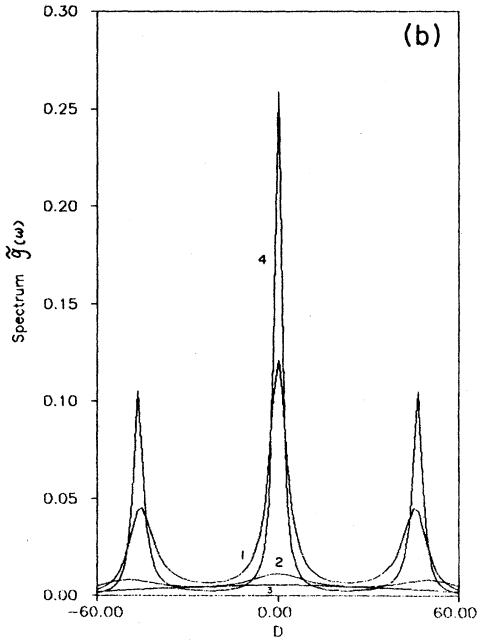

FIG. 8. Resonance fluorescence spectrum. $\Delta=2.0$, $|\Omega|=45.0$, $\epsilon_A=1-\omega_p^2/(\omega^2+i\omega\Gamma_p)$, $\Gamma_p=0.01\omega_P$, $\epsilon_B=3.0$, $\hat{d}_A=0.1$, $\hat{d}_B=0.5$, $x=\omega/\omega_p$. (a) Curve 1, $x=0.1$; curve 2, $x=0.2$; curve 3, $x=0.3$; curve 4, $x=0.4$. (b) Curve 1, $x=0.5$; curve 2, $x=0.7$; curve 3, $x=0.9$; curve 4, $x=1.0$.

We know that both γ and Ω^s are determined by the dielectric properties and geometry of the solid substrate. Therefore the incoherent part of the resonance fluorescence spectrum for an adatom near a surface of a superlattice is also determined by the properties and geometry of this film via both γ and Ω^s. Some of the results calculated numerically from Eqs. (3.1), (3.2), and (4.1) are shown in Figs. 7 and 8, where $\epsilon=1.2$, $\hat{d}=0.3$, and all parameters with dimension t^{-1} are in the unit of γ^0. These figures show how the shape of the spectrum depends on the structure and dielectric properties of the superlattice substrate. From Fig. 7 one can see that different thicknesses of each layer of medium A lead to different number of peaks, positions of sidebands, and heights and half-width of the peaks. In the one-peak case (see curve 2) the effects of nonradiative energy transfer to the surface plasmon become very strong so that more energy of the incident field is absorbed by the surface via the adatom and subsequently the scattered field intensity is too weak to create the sidebands of the spectrum.

Figure 8 shows the dependence of the spectrum on the ratio x of adatomic transition frequency to plasmon frequency of the metal medium A when B is a dielectric. The energy transfer from the excited adatom to the superlattice is strongly dependent on the ratio x. This process can be an effective decay channel for this adatom. For certain x, this process becomes very strong, causing the peaks in the spectrum to merge into the central peak or even disappear. While in other circumstances the above process is weak, there appear three peaks which are higher and narrower.

V. TIME EVOLUTION OF THE ADATOMIC INVERSION

In the interaction of laser with the adatom, when the intensity of the laser is weak, it is more probable for the adatom to stay in the lower state than in the upper state. In this case we approximately have

$$\langle S^z(t)\rangle=-\tfrac{1}{2}\ . \tag{5.1}$$

So, as in Ref. 34, we can linearize the SBE (2.23) to obtain the equations for $\langle S^-(t)\rangle$ and $\langle S^+(t)\rangle$, e.g.,

$$\frac{d}{dt}\langle S^-(t)\rangle=-[i(\Delta+\Omega^s)+\gamma]\langle S^-(t)\rangle\frac{i}{2}\Omega^*\ . \tag{5.2}$$

Inserting (5.2) and its conjugation into the equation of $\langle S^z(t)\rangle$ in the SBE and considering the adatom initially in the lower state, i.e., $\langle S^z(0)\rangle=-\frac{1}{2}$, one can easily obtain

$$\langle S^z(t)\rangle=|\Omega|^2[1+e^{-2\gamma t}-2e^{-\gamma t}\cos(\Delta+\Omega^s)t]/4|z|^2-\tfrac{1}{2}\ . \tag{5.3}$$

With Eq. (5.3) we numerically analyzed time evolution of mean value of the inversion operator and some results are

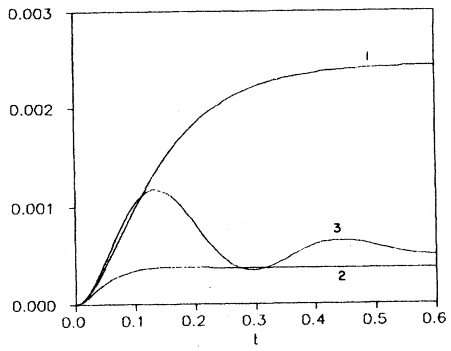

FIG. 9. $[\langle S^z(t)\rangle+\frac{1}{2}]/|\Omega|^2$ vs times t. $\Delta=2.0$, $\epsilon_A=-10.5+0.5i$, $\epsilon_B=3.0$, $\hat{d}_B=0.2$. Curve 1, $\hat{d}_A=0.04$; curve 2, $\hat{d}_A=0.06$; curve 3, $\hat{d}_A=0.25$.

shown in Figs. 9 and 10, where time t is in the unit of $1/\gamma^0$ and $\hat{d}=0.3$. We have found, in general, two lifetimes of a surface-free atom after switching on the exciting laser field, the interaction between the adatom and the field reaches its steady state, and that in the case of stronger energy-transfer process between the adatom and the surface plasmon this interaction goes faster into the steady state and the population of the upper adatomic level decreases. These figures reflect the dielectric effect and size or structure effect of the superlattice substrate.

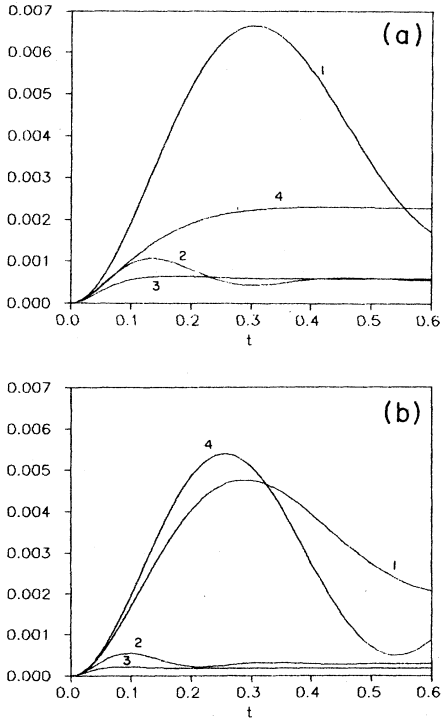

FIG. 10. $(\langle S^z(t)\rangle+\frac{1}{2})/|\Omega|^2$ vs t, $\Delta=2.0$, $\hat{d}_A=0.1$, $\hat{d}_B=0.5$, $\epsilon_A=1-\omega_p^2/(\omega^2+i\omega\Gamma_p)$, $\epsilon_B=3.0$, $\Gamma_p=0.01\omega_p$. (a) Curve 1, $x=0.1$; curve 2, $x=0.2$; curve 3, $x=0.3$; curve 4, $x=0.4$. (b) Curve 1, $x=0.5$; curve 2, $x=0.7$; curve 3, $x=0.9$; curve 4, $x=1.0$.

VI. FLUCTUATIONS OF THE ADATOMIC DIPOLE MOMENT

Very recently, more and more interest has been centered around the generation of squeezed states, due to their potential applications to gravity-wave detection and improved signal-to-noise ratio in light-wave communications.[47,48,65–73] In this section we study squeezing effects in the adatomic operators for the adatom driven by external laser field.

It is known that the dispersive and the absorptive components of the adatomic dipole moment are[46]

$$\sigma_1=(S^+ +S^-)/2 , \tag{6.1}$$

$$\sigma_2=(S^+ -S^-)/2i , \tag{6.2}$$

respectively. Letting $\sigma_3=S^z$, we have the commutation relation

$$[\sigma_1,\sigma_2]=i\sigma_3 \tag{6.3}$$

and the corresponding uncertainty relation

$$(\Delta\sigma_1)^2(\Delta\sigma_2)^2\geq\langle\sigma_3\rangle^2/4 . \tag{6.4}$$

Hence, the adatomic state is said to be squeezed when one of the operators σ_1 and σ_2 satisfies the relation[48]

$$(\Delta\sigma_i)^2<|\langle\sigma_3\rangle|/2, \quad i=1,2 \tag{6.5}$$

and the adatom is said to be in the coherent state when both σ_1 and σ_2 satisfy

$$(\Delta\sigma_i)^2=|\langle\sigma_3\rangle|/2 . \tag{6.6}$$

It is known that the statistical properties of the radiation field are directly related to those of the atomic dipole moment operator. Therefore the occurrence of squeezing may be studied by examining the reduced fluctuations in the adatomic dipole moment.

With Eqs. (2.23), (6.1), and (6.2) we have the steady-state results:

$$(\Delta\sigma_1)^2=[1-(\Delta+\Omega^s)^2|\Omega|^2/(|\Omega|^2/2+|z|^2)^2]/4 , \tag{6.7}$$

$$(\Delta\sigma_2)^2=[1-\gamma^2|\Omega|^2/(|\Omega|^2/2+|z|^2)^2]/4 , \tag{6.8}$$

$$\langle\sigma_3\rangle=-|z|^2/2(\tfrac{1}{2}|\Omega|^2+|z|^2) . \tag{6.9}$$

Putting

$$Q_i=(\Delta\sigma_i)^2-|\langle\sigma_3\rangle|/2, \quad i=1,2 \tag{6.10}$$

we may rewrite the condition (6.5) as

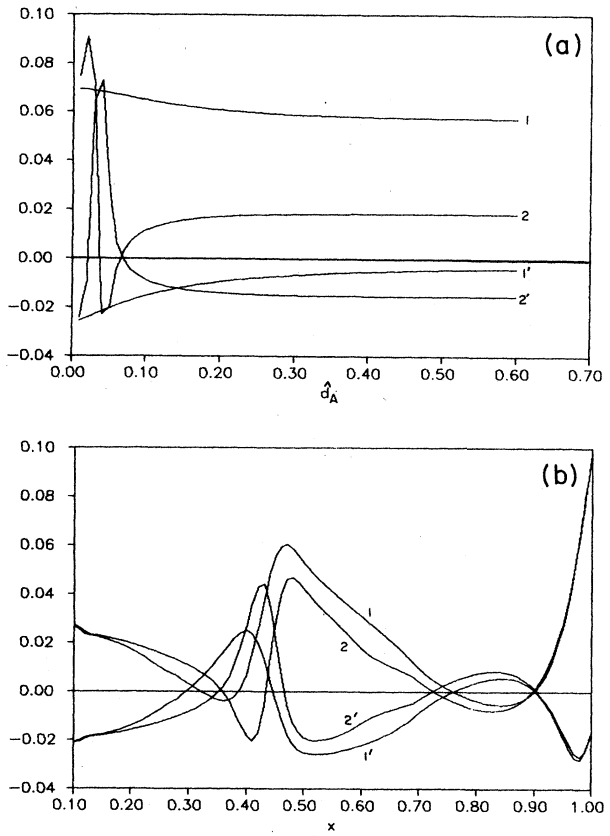

FIG. 11. $\Delta=5.0$, $|\Omega|=10.0$, $\hat{d}=0.3$, $\epsilon_B=3.0$. (a) Q_1 and Q_2 vs $\hat{d}_A$, $\hat{d}_B=0.2$; curve 1 (Q_2) and curve 1′ (Q_1), $\epsilon_A=1.96+1.06i$; curve 2 (Q_2) and curve 2′ (Q_1), $\epsilon_A=10.5+0.5i$. (b) Q_1 and Q_2 vs x, $\epsilon_A=1-\omega_p^2/(\omega^2+i\omega\Gamma_p)$, $\Gamma_p=0.01\omega_p$, $\hat{d}_A=0.1$. Curve 1 (Q_2) and curve 1′ (Q_1), $\hat{d}_B=0.2$; curve 2 (Q_2) and curve 2′ (Q_1), $\hat{d}_B=0.5$.

$$Q_1<0 \tag{6.11}$$

for squeezing in the dispersive component of the dipole moment and

$$Q_2<0 \tag{6.12}$$

for squeezing in the absorptive component.

Figure 11 shows some numerical results calculated from Eqs. (6.7)–(6.10) in the case of strong excitation. It is evident that the fluctuations in the adatomic dipole moment strongly depend on the structure and properties of the substrate. When medium A is a metal, there exhibits alternative squeezing in σ_1 or σ_2. For certain values of ω/ω_p, the Q_1 curve and Q_2 curve intersect simultaneously with the x axis. This means that the adatom is in the coherent state. These interesting phenomena result from the complicated nonlinear coupling of the adatom with the surface-reflected field and the exciting laser field. We know that in the surface-free case[48] there are only two factors, i.e., Δ and Ω, to be properly chosen to create squeezing. However, in the present problem the adatom near a solid surface emits radiation field, which is partially reflected by the surface, accompanied by nonradiative energy transfer to the surface. The reflected field in turn acts back on this adatom and influences its dynamic behavior and statistical properties. The energy-transfer process and the phase and amplitude of the reflected field depend on the structure and properties of the substrate. Therefore, it is doubtless that besides Δ and Ω, fluctuations of the dipole moment of this adatom strongly depend on the dielectric properties, modulation length, etc. of this superlattice.

VII. SUMMARY

In this paper we have solved Maxwell equations and the surface-dressed optical Bloch equations for the interaction of light with an adatom near a surface of a semi-infinite superlattice with periodic structure. Many novel phenomena have been revealed for the first time. In the existing relevant literature, attention is usually paid to the effects of the distance between the adatom and the solid surface. However, here we are particularly interested in the effects of structures and dielectric properties of the superlattice substrate. Studies on the quasiperiodic structure of the superlattice substrate are now underway and will be reported on in the near future.

[1]A. Otto, Surf. Sci. **75**, L392 (1978).
[2]T. H. Wood and M. V. Klein, J. Vacuum Sci. Technol. **16**, 459 (1979).
[3]B. Pettinger and U. Wenig, Chem. Phys. Lett. **56**, 253 (1978).
[4]T. E. Furtak, Solid State Commun. **28**, 903 (1978).
[5]C. Y. Chen and E. Burstein, Bull. Am. Phys. Soc. **24**, 341 (1979).
[6]J. C. Tsang and J. Kirtley, Solid State Commun. **30**, 617 (1979).
[7]S. Efrima and H. Metiu, J. Chem. Phys. **70**, 2297 (1979).
[8]S. Efrima and H. Metiu, Surf. Sci. **92**, 433 (1980).
[9]R. Fuchs, Bull. Am. Phys. Soc. **24**, 339 (1979).
[10]T. E. Furtak and J. Reyes, Surf. Sci. **93**, 351 (1980).
[11]D. A. Weitz, S. Garoff, J. I. Gersten, and A. Nitzan, J. Chem. Phys. **78**, 5324 (1983).
[12]G. C. Schatz, *Surface-Enhanced Raman Scattering* (Plenum, New York, 1983), p. 35.
[13]P. Das and H. Metiu, J. Phys. Chem. **89**, 4681 (1985).
[14]K. H. Drexhage, J. Lumin. **1-2**, 693 (1970); *Progress in Optics* (North-Holland, Amsterdam, 1974), Vol. XII, 165.
[15]H. Morawitz, Phys. Rev. **187**, 1792 (1969).
[16]H. Kuhn, J. Chem. Phys. **53**, 101 (1970).
[17]K. H. Tews, Ann. Phys. (Leipzig) **29**, 97 (1973).
[18]R. R. Chance, A. Prock, and R. Silbey, J. Chem. Phys. **60**, 2184 (1974); **60**, 2744 (1974); **62**, 2245 (1975); Phys. Rev. A **12**, 1448 (1975); Solid State Commun. **18**, 1259 (1976).
[19]G. S. Agarwal, Phys. Rev. Lett. **32**, 703 (1974); Phys. Rev. A **11**, 230 (1975); **11**, 243 (1975); **11**, 253 (1975); **12**, 1475 (1975); Opt. commun. **42**, 205 (1982).
[20]R. R. Chance, A. H. Liller, A. Prock, and R. Silbey, Chem. Phys. Lett. **33**, 590 (1975); J. Chem. Phys. **63**, 1589 (1975).

[21]P. W. Milonni and P. L. Knight, Opt. Commun. **9**, 119 (1973).
[22]R. R. Chance, A. Prock, and R. Silbey, Adv. Chem. Phys. **37**, 1 (1978).
[23]W. H. Weber and C. F. Eagen, Opt. Lett. **4**, 236 (1979).
[24]G. S. Agarwal and H. D. Vollmer, Phys. Status Solidi B **79**, 249 (1977); **85**, 301 (1978).
[25]R. Ruppin, J. Chem. Phys. **76**, 1681 (1982).
[26]J. L. Gersten and A. Nitzan, J. Chem. Phys. **73**, 3023 (1980); **75**, 1139 (1981).
[27]G. S. Agarwal and C. V. Kunasz, Phys. Rev. B **26**, 5832 (1982).
[28]P. K. Aravind and H. Metiu, Surf. Sci. **124**, 506 (1983).
[29]P. M. Whitmore, A. P. Alivisatos, and C. B. Harris, Phys. Rev. Lett. **50**, 1092 (1983).
[30]W. R. Holland and D. G. Hall, Phys. Rev. Lett. **52**, 1041 (1984).
[31]K. C. Liu and Thomas F. George, Phys. Rev. B **32**, 3622 (1985).
[32]R. Rossetti and L. E. Brus, J. Chem. Phys. **76**, 1146 (1982).
[33]A. P. Alivisatos, D. H. Waldeck, and C. B. Harris, J. Chem. Phys. **82**, 541 (1985).
[34]X. Y. Huang, J. T. Lin, and T. F. George, J. Chem. Phys. **80**, 893 (1984).
[35]X. Y. Huang and T. F. George, J. Phys. Chem. **88**, 4801 (1984).
[36]X. Y. Huang, K. C. Liu, and T. F. George, *Laser-Controlled Chemical Processing of Surface* (Elsevier, New York, 1984); Mater. Res. Soc. Symp. Proc. **29**, 381 (1984).
[37]X. Y. Huang, T. F. George, and J. T. Lin, *Coherence and Quantum Optics V* (Plenum, New York, 1984), p. 685.
[38]X. Y. Huang, K. T. Lee, and T. F. George, J. Chem. Phys. **85**, 567 (1986).
[39]J. T Lin, X. Y. Huang, and T. F. George, J. Opt. Soc. Am. B **4**, 219 (1987).
[40]X. S. Li and C. D. Gong, Phys. Rev. A **35**, 1595 (1987).
[41]H. Kuhn, Pure Appl. Chem. **11**, 345 (1965); Naturwissenschaften **54**, 429 (1967).
[42]H. Kuhn, D. Mobius, and H. Bucher, *Physical Methods of Chemistry* (Wiley, New York, 1972), Vol. 1, Pt. 3B, p. 577.
[43]K. H. Drexhage, H. Kuhn, and F. P. Schofer, Ber. Bunsenges. Phys. Chem. **72**, 329 (1968).
[44]K. H. Drexhage, Sci. Am. **222**, 108 (1970).
[45]B. R. Mollow, Phys. Rev. **188**, 1969 (1969); Phys. Rev. A **15**, 1023 (1977); *Dissipative Systems in Quantum Optics* (Springer-Verlag, New York, 1982), Chap. 2.
[46]L. Allen and J. H. Eberly, *Optical Resonance and Two-Level Atoms* (Wiley, New York, 1975).
[47]J. H. Eberly and P. W. Milonni, Encycl. Phys. Sci. Technol. (Academic, New York, 1987), Vol. 11, p. 471; X. Y. Huang, R. Tanas, and J. H. Eberly, Phys. Rev. A **26**, 892 (1982).
[48]D. F. Walls and P. Zoller, Phys. Rev. Lett. **47**, 709 (1981).
[49]J. H. Eberly, Quantum Optics with Very Intense Lasers, a lecture presented at the Workshop on Lasers and Laser Spectroscopy, Kanpur, 1987 (unpublished).
[50]K. Wodkiewicz and J. H. Eberly, Phys. Rev. A **31**, 2314 (1985).
[51]P. L. Knight and P. W. Milonni, Phys. Rep **66**, 21 (1980).
[52]G. S. Agarwal, *Quantum Statistical Theories of Spontaneous Emission and their Relation to Other Approaches,* Vol. 70 of *Springer Tracts in Modern Physics* (Springer-Verlag, New York, 1974).
[53]M. Yamanoi and J. H. Eberly, Phys. Rev. Lett. **52**, 1353 (1984); J. Opt. Soc. Am. B **1**, 751 (1984).
[54]K. Wodkiewicz and J. H. Eberly, Phys. Rev. A **32**, 992 (1985).
[55]J. T. Lin, X. Y. Huang, and T. F. George, Solid State Commun. **47**, 63 (1983).
[56]H. Dekker, Physica A **95**, 311 (1979).
[57]L. S. Zhang, Physica A **117**, 355 (1983).
[58]Z. Q. Zheng, C. M. Falco, J. B. Ketterson, and I. K. Schuller, Appl. Phys. Lett. **38**, 424 (1981).
[59]R. E. Camley, T. S. Rahman, and D. L. Mills, Phys. Rev. B **27**, 261 (1983).
[60]P. Grunberg and R. Mika, Phys. Rev. B **27**, 2955 (1983).
[61]R. E. Camley and D. L. Mills, Phys. Rev. B **29**, 1695 (1984).
[62]L. Z. Zhou and C. D. Gong (unpublished).
[63]G. S. Agarwal and S. V. Oneil, Phys. Rev. B **28**, 487 (1983).
[64]M. Sargent, M. O. Scully, and W. E. Lamb, Laser Physics (Addison-Wesley, Reading, Mass., 1974), Chap. 17.
[65]J. A. Vaccaro and D. T. Pegg, J. Mod. Opt. **34**, 855 (1987).
[66]J. E. Carrol, Opt. Acta **33**, 909 (1986).
[67]S. Machida, Y. Yamamoto, and Y. Itaya, Phys. Rev. Lett. **58**, 1000 (1987).
[68]J. Gea-Banacloche and G. Leuchs, J. Mod. Opt. **34**, 793 (1987).
[69]C. W. Gardiner, Phys. Rev. Lett. **56**, 1917 (1986).
[70]H. J. Carmichael, A. S. Lane, and D. F. Walls, J. Mod. Opt. **34**, 821 (1987).
[71]G. J. Milburn, Phys. Rev. A **34**, 4882 (1986).
[72]B. Yurke and E. A. Whittaker, Opt. Lett. **12**, 236 (1987).
[73]R. Loudon and P. L. Knight, J. Mod. Opt. **34**, 709 (1987).